ACS Catalysis

Research Article

pubs.acs.org/acscatalysis

Versatile Nickel–Lanthanum(III) Catalyst for Direct Conversion of Cellulose to Glycols

Ruiyan Sun,[†,‡] Tingting Wang,[§] Mingyuan Zheng,*[,†] Weiqiao Deng,*[,§] Jifeng Pang,[†] Aiqin Wang,[†] Xiaodong Wang,[†] and Tao Zhang*[,†]

[†]State Key Laboratory of Catalysis, Dalian Institute of Chemical Physics, Chinese Academy of Sciences, Dalian 116023, China,

[§]State Key Laboratory of Molecular Reaction Dynamics, Dalian National Laboratory for Clean Energy, Dalian Institute of Chemical Physics, Chinese Academy of Sciences, Dalian 116023, China

[‡]Graduate University of Chinese Academy of Sciences, Beijing 100049, China

Supporting Information

ABSTRACT: Using cellulosic biomass to synthesize bulk quantities of high-value chemicals is of great interest for developing a sustainable biobased society. Especially, direct catalytic conversion of cellulose to glycols, important building blocks for polymers, remains a grand challenge. Herein, we report the development of a versatile binary nickel–lanthanum(III) catalyst for the conversion of cellulose to both ethylene glycol (EG) and propylene glycol (1,2-PG) in a yield of 63.7%, which is one of the best performances reported for this catalytic reaction. Especially, lanthanum(III) exhibited a high level of activity toward the degradation of cellulose (TON = 339) at a very low concentration (0.2 mmol/L). On the basis of density functional theory calculations and experimental analyses, we addressed a dual route for this catalytic mechanism: a major route involving the selective cracking of sugars into C_2 molecules and a minor route involving the hydrogenolysis of sugar alcohols. Lanthanum(III) catalyzes the cleavage of the C2–C3 bond in glucose via sequential epimerization and 2,3-hydride shift reactions to form glycolaldehyde, the precursor of EG.

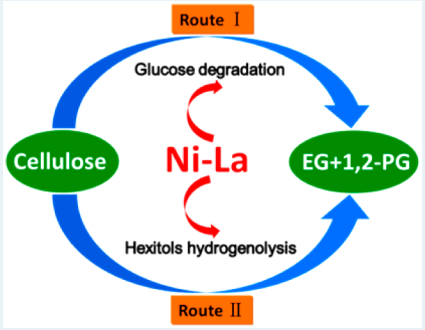

KEYWORDS: *cellulose, ethylene glycol, propylene glycol, nickel–lanthanum catalyst, dual route, theoretical calculation*

INTRODUCTION

The ever-diminishing reserves of fossil energy resources and increasing levels of energy consumption will ultimately result in global energy shortages and serious environmental problems. The conversion of cellulose into chemicals and fuels could play an important role in averting these problems, and research toward this goal has grown considerably during the past decade.[1−3] Efficient reaction processes and catalysts for the selective degradation of cellulose, however, have been difficult to identify because of the robust crystalline structure and high chemical stability of cellulose,[4−6] and further work is therefore needed to explore this area in greater detail. Among the variety of chemical conversions reported for cellulose,[1,7−11] its catalytic transformation to ethylene glycol (EG) and 1,2-propylene glycol (1,2-PG) by hydrolytic hydrogenation represents a particularly attractive process because of its high atomic economy, value-added products and large market demand.[12−16]

Glycols are widely used in the synthesis of a broad range of materials, including polyester, antifreezing agents, and chemical intermediates.[12] For EG, in particular, the world capacity is forecasted to expand from 28 million tons in 2011 to 36 million by 2016.[17]

A breakthrough in the conversion of cellulose to EG and 1,2-PG was achieved in 2008, with further developments being reported in the years that followed. When the cellulose conversion process was conducted in the presence of a series of tungstenic catalysts, including Ni–W_2C, WP, Ni–W, WO_3, and Ru/AC-H_2WO_4, the EG yields reached unprecedented levels of 49.8–69.5% (carbon yield).[13,14,18−23] The use of both heterogeneous tungstenic catalysts, such as tungsten carbides and bimetallic catalysts,[13,22] and homogeneous tungstenic catalysts in combination with hydrogenation catalysts, such as Raney Ni–H_2WO_4 and Ru/AC-ammonium metatungstate,[24,25] has been reported to provide enhanced levels of performance with regard to the conversion of cellulose. The tungstenic species that dissolve in water during the reaction have been found to be catalytically active toward the degradation of sugars via a retro-aldol condensation to form glycolaldehyde, which is a precursor of EG.[15,19] However, once sugars have been hydrogenated to the corresponding hexitols, they become so chemically stable that they cannot be degraded to C_2 molecules by the tungstenic catalysts.[15,22] With this in mind, an ideal catalyst for the production of glycols from cellulose would therefore need to perform two functions concurrently, including the degradation of sugars and the degradation of the resulting hexitols.

Received: September 11, 2014
Revised: November 24, 2014
Published: December 16, 2014

© 2014 American Chemical Society

DOI: 10.1021/cs501372m
ACS Catal. 2015, 5, 874–883

Besides tungstenic catalysts, several researchers have recently explored the use of other catalysts for the conversion of cellulose to glycols, including Ni/ZnO and Cu/Cr_2O_3. Disappointingly, however, these catalysts provided relatively low yields of EG (19.1−28.9%), with 1,2-PG being formed as the main product (34.4−47.6%).[26,27] Given that the market capacity for EG is 1 order of magnitude higher than that of 1,2-PG, catalysts with a high level of selectivity for EG would be much more attractive for the conversion of cellulose to glycols. Furthermore, the reaction mechanism for the conversion of cellulose to EG over these catalysts has not yet been elucidated at the molecular level.

Significant research efforts have been directed toward the use of homogeneous catalysts for the conversion of biomass into useful materials,[28] as exemplified by the isomerization of glucose to fructose by Al(III) and Cr(III),[29,30] the conversion of fructose to 5-hydroxymethyl furfural with Cr(III),[29,31] and the degradation of cellulose to lactic acid in the presence of Pb(II).[32] There are many unique advantages associated with the use of homogeneous catalysts, including high reaction activity and selectivity, enhanced accessibility to catalytically active sites for bulky reactants such as the natural polymer of cellulose, and the simplicity with which the reaction mechanisms of these processes can be studied using computational methods.[31,32] The use of homogeneous catalysis in combination with heterogeneous catalysis could lead to significant improvements in reaction efficiency,[33] a reduction in catalyst costs and allow for the exploration of novel reaction processes.[24,25] Herein, we disclose a versatile binary catalyst, involving the combination of homogeneous lanthanum(III) with a heterogeneous nickel catalyst, which produced EG and 1,2-PG in an overall yield of 63.7% (73.2% of which was EG) from a cellulose conversion process. It is noteworthy that the current Ni−La(III) catalyst exhibited a dual-route reaction mode to produce EG. Furthermore, the concentration of La(III) in the solution could be reduced to an extraordinarily low level of 0.2 mmol/L, which is only 1/6 of the amount of tungstenic catalyst required to give a similarly high yield of EG,[19] not to mention that the price of the La(III) catalyst is just 1/3 of that of the tungstenic catalyst. In light of these results, this newly developed Ni−La(III) catalyst represents a cost-effective, practicable and affordable method for the conversion of cellulose to EG. On the basis of theoretical calculations and correlations with the experiment results, we have also disclosed a mechanism to describe the way in which the catalytic La(III) species facilitates the catalytic retro-aldol condensation of glucose to allow for the formation of EG.

METHODS

Preparation of Catalysts. Lanthanum hydroxide ($La(OH)_3$), nickel nitrate hexahydrate ($Ni(NO_3)_2{\cdot}6H_2O$), cobalt nitrate hexahydrate ($Co(NO_3)_2{\cdot}6H_2O$), barium nitrate ($Ba(NO_3)_2$), D-(+)-glucose, and zirconium nitrate pentahydrate ($Zr(NO_3)_4{\cdot}5H_2O$) were purchased from Sinopharm Chemical Reagent Co. Ferric nitrate nonahydrate ($Fe(NO_3)_3{\cdot}9H_2O$), lanthanum nitrate hexahydrate ($La(NO_3)_3{\cdot}6H_2O$), lanthanum chloride heptahydrate ($LaCl_3{\cdot}7H_2O$), lanthanum hexaboride (LaB_6), lanthanum acetate ($La(OAc)_3{\cdot}nH_2O$), yttrium nitrate hexahydrate ($Y(NO_3)_3{\cdot}6H_2O$), D-1-^{13}C-glucose, and lead nitrate ($Pb(NO_3)_2$) were purchased from Aladdin Chemical Co. Zinc nitrate hexahydrate ($Zn(NO_3)_2{\cdot}6H_2O$), chromic nitrate nonahydrate ($Cr(NO_3)_3{\cdot}9H_2O$), strontium nitrate ($Sr(NO_3)_2$), manganous nitrate ($Mn(NO_3)_2$, 50% aqueous solution), cerium nitrate hexahydrate ($Ce(NO_3)_3{\cdot}6H_2O$), and aluminum nitrate nonahydrate ($Al(NO_3)_3{\cdot}9H_2O$) were purchased from Kermel Chemical Reagent Co. Lanthanum triflate ($La(CF_3SO_3)_3$) was purchased from Alfa Aesar. D_2O was purchased from Qingdao Tenglong Weibo Technology Co.. Lanthanum oxide (La_2O_3) was prepared by the calcination of $La(OH)_3$ at 1123 K in air for 5 h. Activated carbon (AC, S_{BET} = 1203 $m^2\ g^{-1}$) was supplied by Beijing Guanghua-Jingke Activated Carbon Co. 10% Ni/AC catalysts were prepared according to the incipient wetness impregnation method using an aqueous solution of $Ni(NO_3)_2$ as a precursor followed by drying at room temperature overnight followed by a period of heating at 393 K for 8 h. The resulting material was then reduced under a stream of H_2 at 523 K for 2 h. Prior to being exposed to air, the catalysts were passivated under a stream of 1% O_2 in N_2 for at least 5 h. 10% Ni-0.5% Ir (Ru)/La_2O_3 was prepared according to the wet impregnation method. In a typical preparation, 0.8 g of nickel nitrate and 0.2 g of a 10% aqueous solution of $RuCl_3$ (H_2IrCl_6) were placed in a 250 mL beaker containing 20 mL of deionized water, followed by 1.5 g of La_2O_3 under continuous stirring. The resulting mixture was then heated to 303 K to allow for the complete evaporation of water. The resulting catalyst was then dried at 393 K for 8 h, calcined at 773 K for 4 h under a stream of N_2 flow, and lastly reduced at 773 K for 5 h under a stream of H_2.

Characterization Methods. X-ray diffraction (XRD) patterns were recorded on a PANalytical PW3040/60 X′ Pert PRO diffractometer equipped with a Cu Kα radiation source (λ = 0.15432 nm), operating at 40 kV and 40 mA. The metals ions in solution after the reaction were determined using inductively coupled plasma atomic emission spectrometry (ICP-AES) on an IRIS intrepid II XSP instrument (Thermo Electron Corporation). Total organic carbon (TOC) analysis was conducted on a Vario EL III element analyzer (Elementar) to determine the carbon content of the liquid products. Transmission electron microscopy analysis was performed on a JEM-2000EX (JEOL) microscope. The CO_2-temperature-programmed desorption (TPD) experiment was conducted on a Micromeritics AutoChem II 2920 automated catalyst characterization system. In detail, a La_2O_3 sample was heated at 773 K for 1 h in an oxygen flow. CO_2 was then dosed several times at 323 K to allow for the adsorption of CO_2 to reach saturation. Physisorbed CO_2 was then removed in a helium stream at 323 K over 20 min. This stage was immediately followed by the CO_2-TPD experiment, which was conducted under a helium flow (20 mL/min) from 323 to 1173 K at a heating rate of 10 K/min, and the resulting signal was recorded with a thermal conductivity detector (TCD). Solution NMR analysis was performed on a Bruker Avance III 400 MHz instrument (Bruker). All of the experiments were conducted in D_2O. Mass and MS/MS spectrometry measurements were performed on an Agilent Techonlogies 6540 Ultra-High-Definition (UHD) Accurate-Mass Q-TOF LC/MS system (Agilent) equipped with an electrospray ionization source operating in the positive ion mode. Electrospray ionization was conducted at 3500 V, and a collision energy of 20 eV was used for the collision-induced dissociation stage in the MS/MS measurements. The MS and MS/MS measurement were conducted over m/z range of 50 to 600.

Catalytic Reaction. The catalytic conversion of cellulose (Merck, microcrystalline with an average particle size of about 90 μm and a specific surface area of 1.7 $m^2\ g^{-1}$) was carried out in a stainless-steel autoclave (Parr Instrument Company) at 5

DOI: 10.1021/cs501372m
ACS Catal. 2015, 5, 874−883

Table 1. Results of Cellulose Conversions with Binary Catalysts of Metal Compounds in Combination with 10%Ni/AC[a]

			yield (%)[c]								
entry	catalyst	conv. (%)[b]	Ery	Gly	EG	1,2-PG	Man	1,2-BD	Sor	$yield_{GC}$ (%)[d]	$yield_{LC}$ (%)[d]
1	blank	87.8	1.9	2.5	9.5	9.8	6.2	5.0	16.6	2.0	74.2
2	$Co(NO_3)_2$	85.4	2.4	3.3	15.6	9.5	6.3	4.2	12.8	3.3	76.2
3	$Fe(NO_3)_3$	87.2	2.2	3.3	14.1	9.5	5.8	3.8	11.9	3.6	75.4
4	$Zn(NO_3)_2$	94.0	3.0	5.9	16.7	12.3	5.7	4.7	5.9	6.0	80.8
5	$Al(NO_3)_3$	85.2	2.2	3.1	15.4	8.8	6.3	4.5	12.2	3.4	74.5
6	$Cr(NO_3)_3$	85.1	1.9	3.2	16.2	9.3	5.7	4.4	11.1	4.6	74.7
7	$Zr(NO_3)_4$	89.1	2.0	3.5	15.5	9.6	5.6	4.3	11.8	3.5	75.8
8	$Mn(NO_3)_2$	91.6	2.0	4.1	16.6	11.7	5.8	4.3	9.9	5.0	77.6
9	$Pb(NO_3)_2$	90.4	1.0	2.0	17.2	12.7	2.8	4.5	5.4	2.5	73.8
10	$Ba(NO_3)_2$	86.6	2.5	4.2	18.0	10.7	5.5	4.7	6.4	6.2	75.4
11	$Sr(NO_3)_2$	90.4	2.2	3.5	17.1	9.4	5.3	3.5	7.9	5.1	74.5
12	$Y(NO_3)_3$	94.8	1.6	4.8	29.5	11.5	1.9	3.3	0.7	7.6	82.4
13	$Ce(NO_3)_3$	92.6	1.2	4.7	30.2	15.6	1.0	4.3	0.6	10.1	71.2
14	$La(NO_3)_3$	95.3	2.1	5.7	32.6	13.8	2.0	4.6	1.6	8.5	78.6
15	$La(OAc)_3$	94.3	1.4	5.0	33.9	13.1	1.0	1.3	1.1	5.0	84.6
16	LaB_6	95.0	1.3	3.7	32.0	15.2	1.1	3.1	3.3	2.7	81.5
17	$LaCl_3$	100	1.1	1.6	20.5	10.0	0.8	0.9	1.4	2.0	71.0
18	$La(OTf)_3$	98.7	1.2	4.2	22.3	8.8	1.0	1.3	0.4	2.6	73.5
19	La_2O_3	95.6	2.2	5.5	36.0	14.7	1.7	3.6	3.3	3.5	84.3
20	$La(OH)_3$	96.6	1.4	5.7	38.4	14.6	1.2	3.2	0.6	5.1	82.2
21	$La(OH)_3$[e]	100	0.7	22.5	25.1	27.3	0	3.9	0	7.4	82.2

[a]Reaction conditions: 0.15 g of 10% Ni/AC, 0.02 mmol metal cation, 0.25 g of cellulose, 25 mL of H_2O, 518 K, 5 MPa of H_2, 120 min, 800 rpm. Ery, Gly, EG, 1,2-PG, Man, 1,2-BD and Sor are abbreviations for erythritol, glycerol, ethylene glycol, 1,2-propylene glycol, mannitol, 1,2-butanediol and sorbitol, respectively. [b]Cellulose conversion (wt %) was calculated by the change of cellulose weight before and after the reaction [c]The yields of polyols were calculated by using the equation: yield (C%) = (masses of carbon in the products)/(masses of carbon in cellulose charged into the reactor) × 100%. [d]$Yield_{GC}$ and $Yield_{LC}$ indicate the total carbon in the gas and liquid products, respectively, and were calculated on the basis of carbon. [e]0.25 g of sorbitol was employed as substrate.

MPa of H_2 pressure (measured at room temperature) and 518 K. For each reaction, 0.25 g of cellulose, a designated amount of catalyst, and 25 mL of deionized water were placed in a 75 mL autoclave, and the resulting mixture was stirred at 800 rpm. For the recycling test, the catalysts were recovered after each run by filtration and washed several times with deionized water before being used in the next reaction together with the same amounts of cellulose and water used in the first run. The liquid-phase products were analyzed by HPLC on an Agilent 1200 system equipped with a Shodex Sugar SC1011 column and a differential refractive index detector (RID). HPLC analysis was conducted at a column temperature of 318 K using water as the mobile phase with a flow rate of 0.6 mL min^{-1}. The samples were injected with an injection volume of 5.0 μL. Gaseous products were analyzed by GC on an Agilent 6890N system equipped with a TDX-1 column and a TCD. Cellulose conversions were determined by measuring the difference in the cellulose weight before and after the reaction. The polyol yields were calculated on the basis of the amount of carbon according to the equation: yield (C%) = (mass of carbon in the products)/(mass of carbon in the cellulose charged into the reactor) × 100%. The carbon content of the cellulose fed into the reactor was 4230 ppm.[21] The yields of EG and 1,2-PG from the cited literature reports have also been presented in the carbon yields.

Computation Methods. All calculations were performed using the Gaussian 09 software package based on the DFT method. The standard 6-31G** basis set was used for the geometry optimizations, frequency calculations, IRC, and single-point energy calculations (the LanL2DZ basis set was employed for La). The solvent effects were considered in the calculations using the PCM model with water as the solvent. The harmonic frequencies at the equilibrium geometries were calculated to confirm the first-order saddle points, local minima on the potential energy surfaces, and the zero-point energy. Correlations between the corresponding imaginary frequency mode and intrinsic reaction coordinate calculations were evaluated to confirm the transition states and the stable structures.

RESULTS AND DISCUSSION

Screening of Catalysts for Cellulose Conversion. A variety of metal salts were initially screened in combination with a 10% Ni/AC catalyst for the cellulose conversion process. As shown in Table 1, compared with the blank experiment involving the use of 10% Ni/AC in isolation (Table 1, entry 1), the addition of different transition metal salts led to significant changes in yields of EG and 1,2-PG. The addition of La(III) salts afforded the highest levels of selectivity of all of the salts tested toward the production of EG and 1,2-PG. Hexitols (22.8% yield) were observed as the major polyol products in the blank experiment, with EG and 1,2-PG being formed in yields of 9.5 (10.8% EG selectivity) and 9.8%, respectively, after 2 h at 518 K (Table 1, entry 1). Pleasingly, however, the addition of La(III) led to a significant increase in the EG yield to 32.6%, which was accompanied by a 3-fold increase in the EG selectivity (i.e., 34.2% vs 10.8%). The 1,2-PG yield also increased to 13.8% (Table 1, entries 1 and 14). The addition of Ce(III) and Y(III) also led to an increase in EG selectivity, which could be attributed to similarities in the chemical properties of the lanthanide elements or elements belonging to group 3 of the periodic table (Table 1, entries 12 and 13). In

DOI: 10.1021/cs501372m
ACS Catal. 2015, 5, 874−883

contrast, none of the other metal salts tested in the current study lead to similar changes in the selectivity of the reaction toward the formation of EG (Table 1, entries 2−11).

The nature of the anion of La(III) salt had a significant impact on the EG yields (Table 1, entries 14−20). For example, nitrate ions were superior to chloride and triflate ions, most likely because the nitrate anions would have decomposed under the reaction conditions. $La(OH)_3$ and La_2O_3 provided the best performances of all of the La(III) salts tested in the current study in terms of their selectivity for EG (Table 1, entries 19 and 20), and $La(OH)_3$ and La_2O_3 were therefore used as the La(III) source in all of the following reactions. The use of these compounds would also eliminate the possibility of the anion of the La(III) salt having an adverse impact on the reaction because these compounds can dissolve in hot-compressed water to release La(III) ions in situ, in a similar manner to a tungsten acid catalyst that we studied previously.[19]

Catalytic Performance of Ni−La(III) for Cellulose Conversion. The effect of the mass ratio of cellulose to $La(OH)_3$ in the reaction is shown in Figure 1. The EG and 1,2-PG yields remained close to 38 and 15%, respectively, as the mass ratio of cellulose/$La(OH)_3$ increased from 2.5 to 100. Surprisingly, the use of only 1 mg of $La(OH)_3$ (0.2 mmol/L La(III)) in the reaction (i.e., a cellulose/$La(OH)_3$ mass ratio is 250) still afforded high levels of conversion with EG and 1,2-PG yields of up to 30.9 and 14.4%, respectively. The TON for the formation of EG and 1,2-PG at this concentration of La(III) was 339. The ability of such an extraordinarily low concentration of La(III) to realize this level of conversion is of remarkable significance for the practical and low cost application of an homogeneous catalyst. Furthermore, the La(III) ions exhibited catalytic activity toward the cellulose conversion, as evidenced by the higher level of cellulose conversion when the reaction was conducted in the presence of increased concentration of La(III).

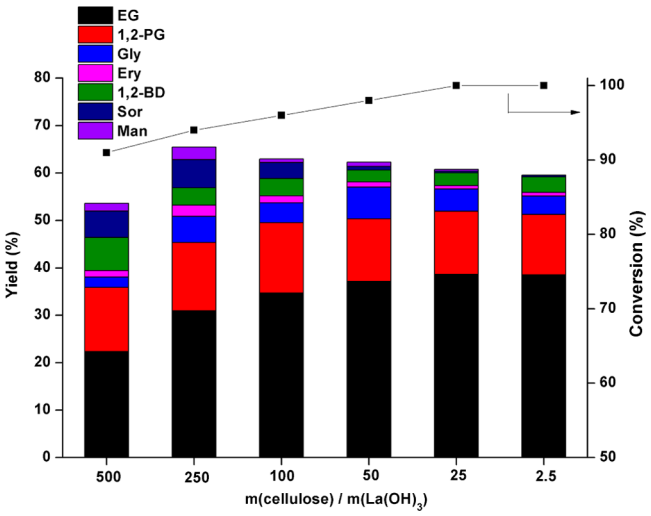

Figure 1. Effect of the mass ratio of cellulose to $La(OH)_3$ on the product yields in the cellulose conversion. Reaction conditions: 518 K, 110 min, 5 MPa of H_2, 800 rpm, 0.15 g of 10% Ni/AC, 0.25 g of cellulose and 25 mL of H_2O.

The effects of the reaction time and temperature on the cellulose conversion are shown in Figure 2a,b. The yields of EG and 1,2-PG increased consistently from the beginning of reaction and eventually reached a plateau around 39 and 13%, respectively. Compared with the Ru/AC-H_2WO_4 catalyst, which realized the complete conversion of cellulose in 30 min,[19] the binary Ni−La(III) catalyst required a longer reaction time to allow for the complete conversion of cellulose. The requirement for a longer reaction time in this case could be related to weaker acidity of Ni−La(III), which would lead to a lower rate of cellulose hydrolysis. Extending the reaction time to 190 min did not lead to a change in the product distribution, which demonstrated that the polyol products were stable to the Ni−La(III) catalyst under the current conditions. The cellulose conversion and the yields of EG and 1,2-PG increased with increasing reaction temperature up to 518 K. At higher temperatures, the hydrogenolysis of the polyols was enhanced to form more gases at the expense of EG and 1,2-PG production.[25]

The stabilities of the different Ni−La(III) catalysts were examined in the recycling experiments, and the results are shown in Figure 3. In the case of 10% Ni/AC-$La(OH)_3$ (Figure 3a), the EG yield decreased remarkably from an initial value of 38.0 to 12.3% after three consecutive runs. The TEM images (Figure 4a,b) and XRD patterns (Figures S1a,b) of the catalysts revealed that the nickel particles on the 10% Ni/AC were significantly sintered after the reaction, which could be attributed to the Ostwald ripening of the Ni particles following their exposure to hot water and a H_2 atmosphere. It is known

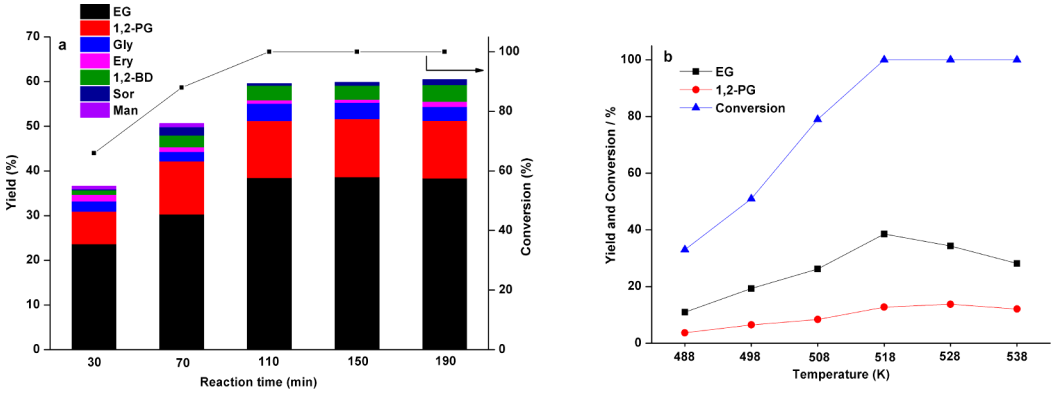

Figure 2. Results of cellulose conversion with the binary catalyst of $La(OH)_3$ and 10%Ni/AC depending on (a) reaction time, reaction temperature: 518 K; (b) reaction temperature, reaction time: 110 min; Reaction conditions: 0.15 g of 10% Ni/AC, 0.1 g of $La(OH)_3$, 0.25 g of cellulose, 25 mL of H_2O, 5 MPa of H_2, 800 rpm.

DOI: 10.1021/cs501372m
ACS Catal. 2015, 5, 874−883

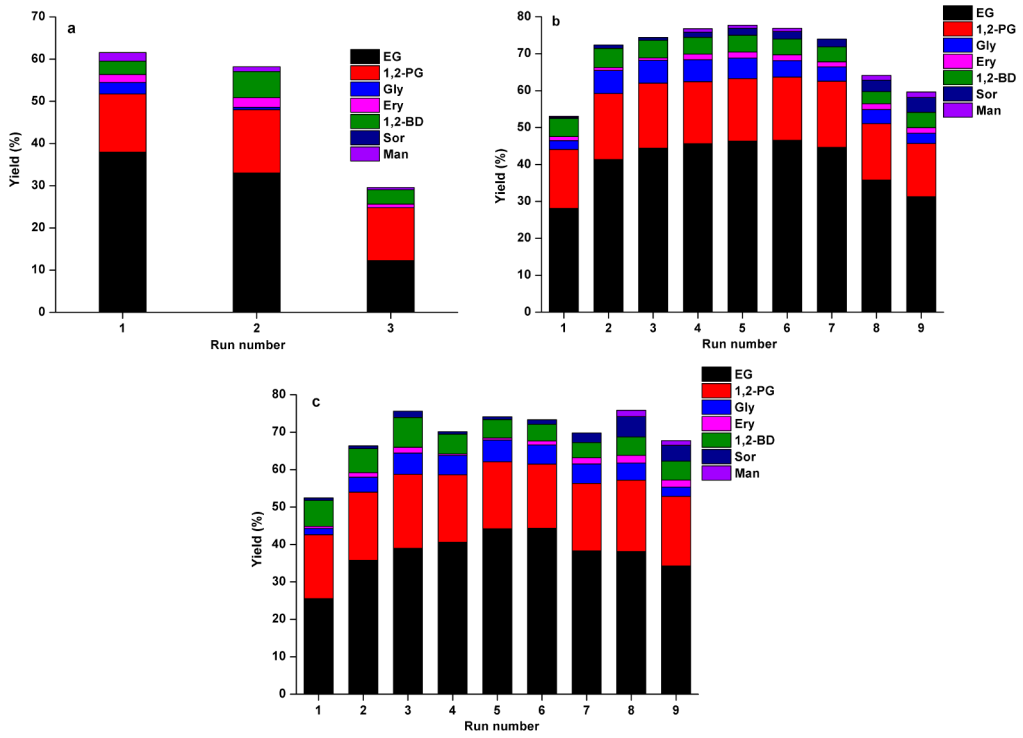

Figure 3. Recycling stabilities of different catalysts in cellulose conversion. (a) 10% Ni/AC-La(OH)$_3$, reaction conditions: 0.15 g of 10% Ni/AC, 0.1 g of La(OH)$_3$, 110 min; (b) 10% Ni-0.5% Ir/La$_2$O$_3$, reaction conditions: 0.15 g of 10% Ni-0.5% Ir/La$_2$O$_3$, 150 min; (c) 10% Ni-0.5% Ru/La$_2$O$_3$, the same reaction conditions as (b). (0.25 g of cellulose, 25 mL of H_2O, 518 K, 5 MPa of H_2, 800 rpm).

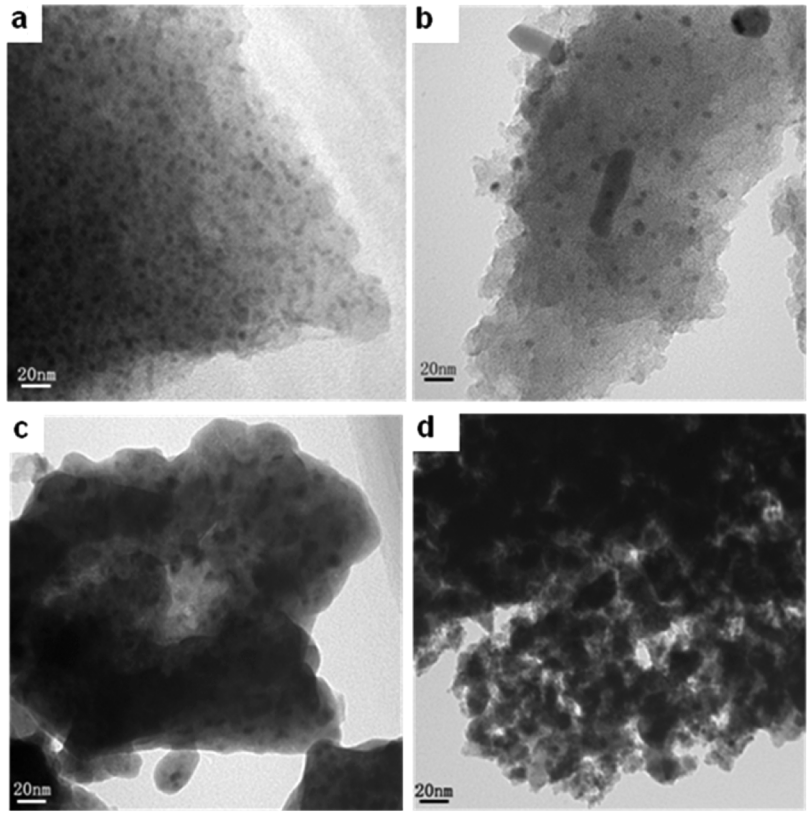

Figure 4. TEM images of fresh and used catalysts: (a) fresh and (b) used 10% Ni/AC, (c) fresh and (d) used 10% Ni-0.5% Ir/La$_2$O$_3$.

that La$_2$O$_3$ can stabilize transition metals when used as a catalyst support or additive.[34−38] The stability of a nickel catalyst can also be improved by the introduction of a small amount of a noble metal.[39,40] With these things in mind, we designed a supported bimetallic catalyst consisting of 10% Ni-0.5% Ir/La$_2$O$_3$ that would simultaneously provide hydro-

DOI: 10.1021/cs501372m
ACS Catal. 2015, 5, 874−883

genation sites and La(III) ions for the reaction. As shown in Figure 3b, the bimetallic catalyst exhibited much greater stability than the previous catalyst over nine cycles. A plot of the polyols yields observed during the recycling experiments revealed that the overall yield of EG and 1,2-PG reached the highest value of 63.7% (73.2% of which was EG) during the sixth run. A similar phenomenon was also observed for the 10% Ni-0.5% Ru/La_2O_3 catalyst (Figure 3c). The concentration of La(III) ions in solution after the reaction was found to be in the range of 100−200 ppm for runs 1−7 (Table S1) meanwhile sintering of nickel particles was not notable, as shown in Figure 4c,d, which demonstrated that La_2O_3 could be used as a suitable support for stabilizing the nickel particles at the same time as releasing La(III) ions in situ for the reaction.

Reaction Pathways. In terms of the reaction mechanisms involved in the conversion of cellulose to EG and 1,2-PG, one possible pathway involving the degradation of hexitols has been studied extensively.[41−46] To determine whether this mechanism was occurring in our reaction, we used sorbitol as substrate in a conditional experiment (Table 1, entry 21). Following a reaction time of 2 h, the sorbitol had been completely degraded to give glycerol, EG and 1,2-PG in yields of 22.5, 25.1 and 27.3%, respectively. This result demonstrated that the Ni−La(III) catalyst was catalytically active toward the conversion of hexitols. This result was therefore consistent with that for the conversion of cellulose in the presence of Ni−La(III) (Table 1, entries 1 and 14−20), where the yields of EG and 1,2-PG increased at the expense of those of the hexitols. The results of a CO_2-desorption experiment on La_2O_3 showed a significant CO_2 desorption peak at 953 K (Figure S2), which indicated that the La(III) salts were becoming basic when they were hydrolyzed in hot water during the reaction.[47] The hexitols could therefore be degraded by the Ni−La(III) catalyst via the same route that occurs in the presence of basic and hydrogenation catalysts. Catalytic behavior of this type from an La(III)-based catalyst is quite different from that of the tungstenic catalysts, which exhibit no activity toward the degradation of hexitols.[15,22]

It is noteworthy, however, that the EG:1,2-PG:Gly product ratio of the sorbitol conversion was 1.1:1.2:1, which is quite different from that of the cellulose conversion, which was 6.7:2.6:1 (Table 1, entries 20 and 21). The Ni−La(III) catalyst demonstrated preferential selectivity for the production of EG in the cellulose conversion process. In this respect, the La(III)-based catalyst behaved like the tungstenic catalyst, which shows an especially high level of selectivity toward the production of EG.

The reaction intermediate glycolaldehyde (GA) was monitored throughout the cellulose conversion process to develop a deeper understanding of the role of La(III) in the degradation of cellulose to EG. When the reaction was conducted in the presence of La(III) and the absence of the Ni catalyst at temperatures above 518 K, the yields of GA were much greater than the yield obtained in the blank experiment (Figure 5). This catalytic behavior of La(III) was very similar to that of the tungstenic catalyst.[19] However, the maximal GA yield achieved by La(III) catalysis was slightly lower than that of the tungstenic catalyst. The starting temperatures for the formation of GA with the La(III) catalysts were also 20 K higher than those of the tungstenic catalysts.[19] This result could therefore account for the lower EG yields observed for the Ni−La(III) catalysts in the cellulose conversion process compared with the tungstenic catalyst.

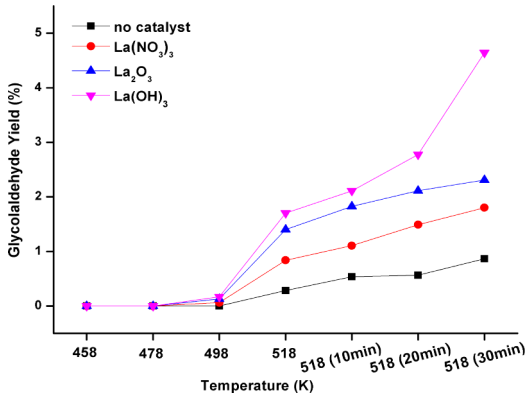

Figure 5. Glycolaldehyde formation in the cellulose conversion over different La(III) compounds without hydrogenation catalyst at 518 K and 5 MPa of H_2 for 30 min.

On the basis of the experimental results described above and our understanding of the mechanisms involved in similar processes,[15] we have proposed a tentative dual-route reaction mode mechanism for the current conversion, which is shown in Scheme 1. During the conversion of cellulose to EG, cellulose would be initially hydrolyzed to glucose and oligosaccharides by the H^+ ions released by the hot water.[11] The resulting sugars would then be converted to EG via two different routes. The first and major route (i) would involve the La(III)-catalyzed degradation of the sugars via a retro-aldol condensation to form GA, which would be hydrogenated over the Ni sites to form EG. The second and minor route (ii) would involve the initial hydrogenation of the sugars to form hexitols, which would undergo a hydrogenolysis reaction to form EG and 1,2-PG.

Reaction Mechanism. Given that extensive studies have been conducted toward developing a deeper understanding of the catalytic degradation of hexitols in the presence of hydrogenation catalysts under basic conditions, we decided to focus exclusively on the mechanism of the proposed dominant route (i). In a similar manner to Pb(II)−OH,[32] Cr(III)−OH,[31] and Sn(IV)−OH,[48,49] La(III) can be hydrolyzed to La(III)−OH in aqueous solution, and this species would have acted as the active species under our current reaction conditions.[50−53] Ultra-High-Definition (UHD) Accurate-Mass Q-TOF LC/MS analysis allowed us to confirm that La(III)−OH was present in the aqueous solutions of La(III) used in the current study (Figure S3). On the basis of this result, La(III)−OH was used to conduct a theoretical calculation to develop a deeper understanding of the way in which La(III) catalyzes the degradation of glucose to GA. The results of this calculation are shown in Figure 6 and Tables S2−22, and a detailed mechanistic explanation to Figure 6 is shown in Scheme S1 as well. In view of these results, it was possible to divide the reaction into four stages, including (i) hydrogen transfer following the formation of a complex between La(III)−OH and glucose; (ii) C2−C3 bond cleavage via sequential glucose epimerization and 2,3-hydride shift reactions; (iii) loss of GA; and (iv) cracking of the erythrose into two molecules of GA.

The initial step would be a hydrogen transfer reaction from C2-OH to La(III)−OH (stage (i). This step would occur quite readily because of its low activation energy ($\Delta G‡$), which was determined to be as low as 0.61 kcal/mol. The length of the C2−O bond would therefore decrease as a consequence of the stronger interactions, which would promote the cleavage of the C2−C3 bond (stage (ii). The cleavage of the C2−C3 bond

DOI: 10.1021/cs501372m
ACS Catal. 2015, 5, 874−883

Scheme 1. Proposed Reaction Pathways for the Conversion of Cellulose to Ethylene Glycol and Propylene Glycol with the Ni–La(III) Catalyst

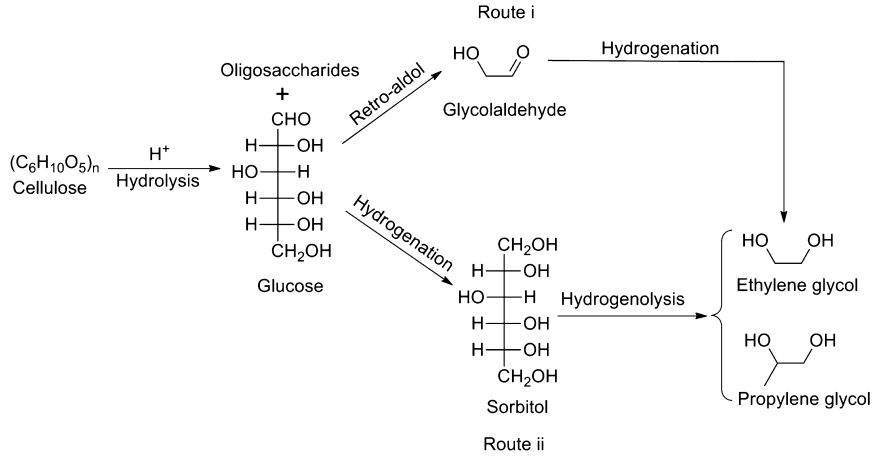

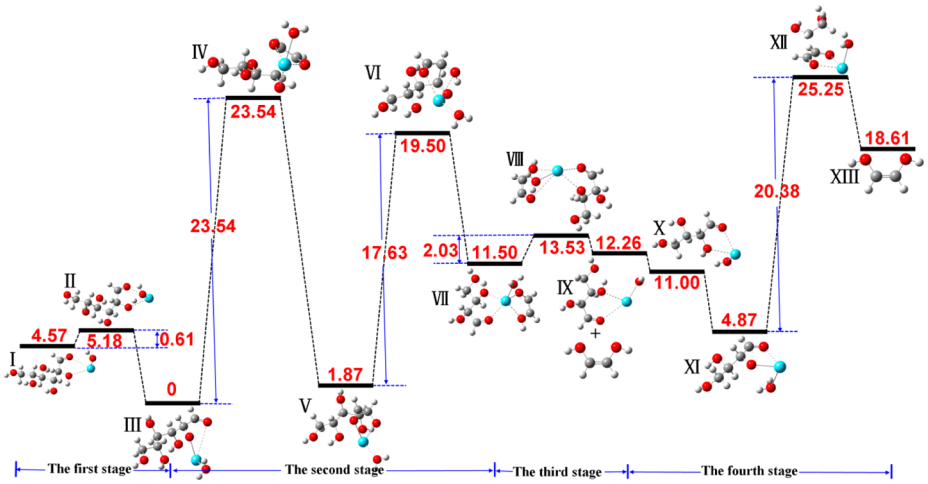

Figure 6. Theoretical calculation for the La(III)–OH-catalyzed conversion of glucose to glycolaldehyde. Calculated Gibbs energy profiles (in kcal/mol) and optimized structures of the species involved in the catalytic process, including intermediates and transition states.

would comprise two steps, including (a) epimerization of glucose with the reversion of C1 and C2 positions and (b) the cleavage of the C2–C3 bond via a 2,3-hydride shift. The $\Delta G‡$ for the first step was determined to be 23.54 kcal/mol, which is the highest activation energy of the four stages. The calculated apparent activation energy of 18.97 kcal/mol (i.e., the difference in the Gibbs energies between I and IV) was very close to the experimental value of 20.0 kcal/mol (Figure S4). This result therefore highlighted the validity of the proposed reaction model. Following the epimerization of glucose, the cleavage of the C2–C3 bond would proceed more readily ($\Delta G‡$ = 17.63 kcal/mol).

GA would be readily formed during stage (iii) via a hydrogen transfer reaction ($\Delta G‡$ = 2.03 kcal/mol). The remaining erythrose would undergo further cracking into two molecules of GA during stage (iv). In contrast to glucose, the C2–C3 bond of erythrose (i.e., the C4–C5 bond of glucose) would break directly following the formation of a stable structure (X) through the torsion of the C–C bonds, and this cleavage process would occur via a hydrogen transfer process in the absence of epimerization. The highest $\Delta G‡$ for this stage was determined to be 20.38 kcal/mol, which is smaller than the value for stage (ii). Stage (iv) would therefore proceed much more readily than stage (ii). This is also consistent with the observed production of much larger quantities of GA during the reaction compared with the erythrose intermediates.

To further confirm the catalytic role of La(III)–OH in the cleavage of the C2–C3 bond of glucose, we compared the energy barriers for the reactions conducted both with and without La(III)–OH. As shown in Figure 7, the $\Delta G‡$ of the reaction conducted in the absence of La(III)–OH was 32.26 kcal/mol, which is notably higher than that of the reaction conducted in the presence of La(III)–OH (23.54 kcal/mol). This result therefore demonstrates that La(III)–OH catalyzes the degradation of glucose to form GA.

Experimental evidence in support of the catalytic function of La(III) in the cleavage of the C2–C3 bond of glucose was provided by the analysis of the reaction solution by tandem mass (MS/MS) spectrometry. The mass (MS) and MS/MS results revealed that the La(III)–glucose complex and the fragments of glucose degradation (i.e., GA and erythrose) were formed via the cleavage of the C2–C3 bond in glucose (Figure 8). In contrast, the analysis of the reaction solution without La(III) revealed no GA or erythrose. Instead, these results revealed the presence of a Na(I)–glucose species as well as several unknown fragments (Figure 9). These results therefore confirmed that glucose was activated by the La(III) species toward selective catalytic degradation.

DOI: 10.1021/cs501372m
ACS Catal. 2015, 5, 874–883

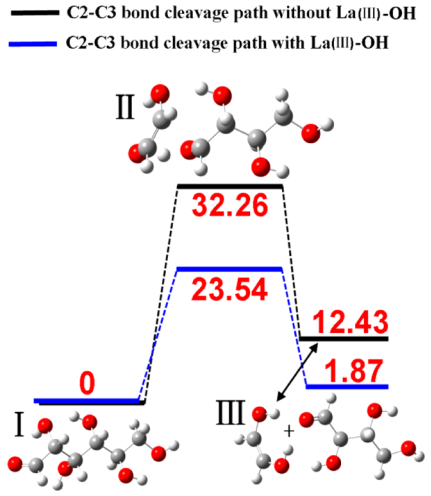

Figure 7. Calculated Gibbs energy profiles (in kcal/mol) and optimized structures of the C2−C3 bond cleavage of glucose with and without La(III)−OH, including intermediates and transition states.

The results of these computational studies confirmed that La(III) catalyzed the cleavage of the C2−C3 bond of glucose through the epimerization of glucose to mannose followed by a 2,3-hydride shift. The epimerization of glucose was confirmed by ^{13}C nuclear magnetic resonance (NMR) experiments using isotopically labeled glucose at C1 (D-1-^{13}C-glucose) as the substrate. ^{13}C NMR analysis of the reaction of D-1-^{13}C-glucose with La(III) following 1 h in deuterium oxide (D_2O) at 413 K revealed a new set of resonance signals at δ_C = 70.7 and 71.3 ppm (Figure 10), which were assigned to the chemical shifts of the α- and β-pyranose units of D-2-^{13}C-mannose, respectively. These results indicated that D-2-^{13}C-mannose was formed via the rearrangement of the carbon skeleton through exchanges at the C1 and C2 positions.[54,55] This result therefore provided further evidence in support of the theoretical calculations. Furthermore, a large amount of D-1-^{13}C-fructose (as evidenced by two new resonances at δ_C = 62.7 and 63.9 ppm corresponding to the α- and β-pyranose units of D-1-^{13}C-fructose, respectively) was also observed in the ^{13}C NMR spectra (Figure 10).[55] This observation was consistent with the HPLC chromatograph (Figure S5) and could be attributed to the isomerization of glucose to fructose, which would be catalyzed by the basic La(III). The computational results showed that the activation energy for the isomerization of glucose isomerization to fructose (18.52 kcal/mol) was lower than that for the epimerization of glucose to mannose (23.54 kcal/mol), which would explain why more fructose was produced by this reaction than mannose (Figure S6). However, the theoretical calculation also showed that the activation energy for the degradation of fructose via the cleavage of its C3−C4 bond was 27.86 kcal/mol, which is higher than that calculated for the degradation of glucose via the cleavage of its C2−C3 bond (23.56 kcal/mol) (Figure S7). This result therefore indicated that the presence of La(III) was advantageous for the degradation of glucose over fructose in terms of the kinetics of the process. This could explain why EG was observed as the dominant product over 1,2-PG under the current reaction conditions.

CONCLUSIONS

In summary, we have developed a versatile binary Ni−La(III) catalyst for the conversion of cellulose to EG and 1,2-PG, which were obtained in a combined yield of 63.7% (with EG accounting for 73.2%). This new Ni−La(III) catalyst is efficient for the degradation of cellulose to EG and 1,2-PG even at the very low La(III) concentration of 0.2 mmol/L. This Ni−La(III) catalyst presents two routes for the production of EG. According to the main route, sugars derived from the hydrolysis of cellulose would be directly degraded to GA with high selectivity by the La(III) catalyst. The GA would then be hydrogenated over the Ni sites to form EG. For the minor route, the sugars would initially undergo a hydrogenation reaction to form hexitols, which would be catalytically degraded to form EG and 1,2-PG by basic La(III) and metallic nickel. Using theoretical calculations, we have clearly shown that glucose undergoes epimerization and 2,3-hydride shift steps in the presence of the La(III) catalyst to form GA, and the results of these computational experiments were in good agreement with the experimental findings.

In contrast to the tungstenic catalysts that have been studied extensively in glucose conversion processes, the current Ni−La(III) catalyst exhibited several attractive features for the

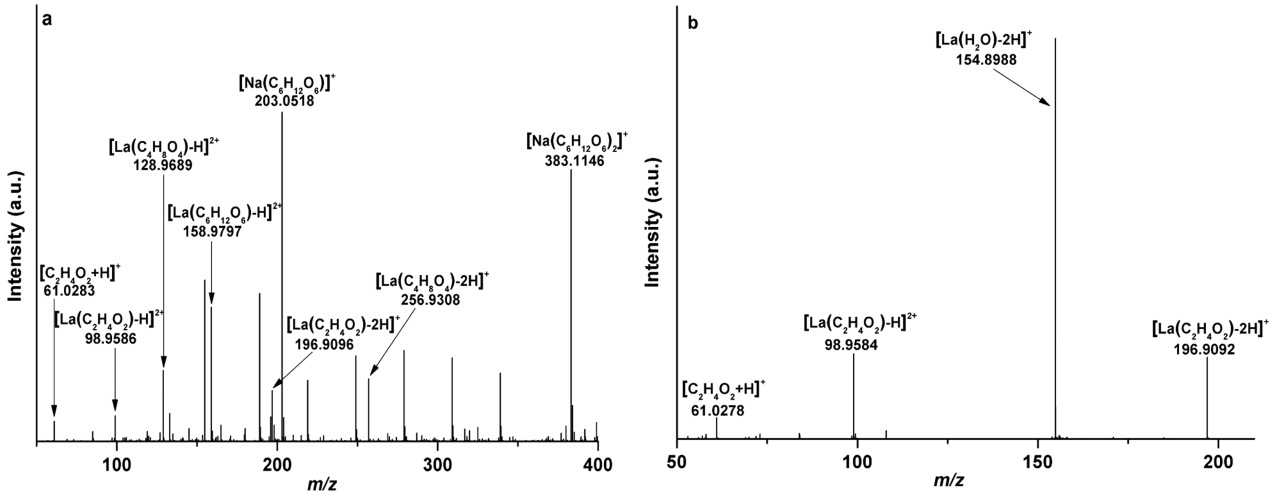

Figure 8. MS and MS/MS spectra of glucose in the presence of La(III). (a) MS spectrum. (b) MS/MS spectrum of the $[La(C_6H_{12}O_6)-H]^{2+}$ species with m/z of 158.9797, which was selected as target ion to conduct MS/MS experiment.

DOI: 10.1021/cs501372m
ACS Catal. 2015, 5, 874−883

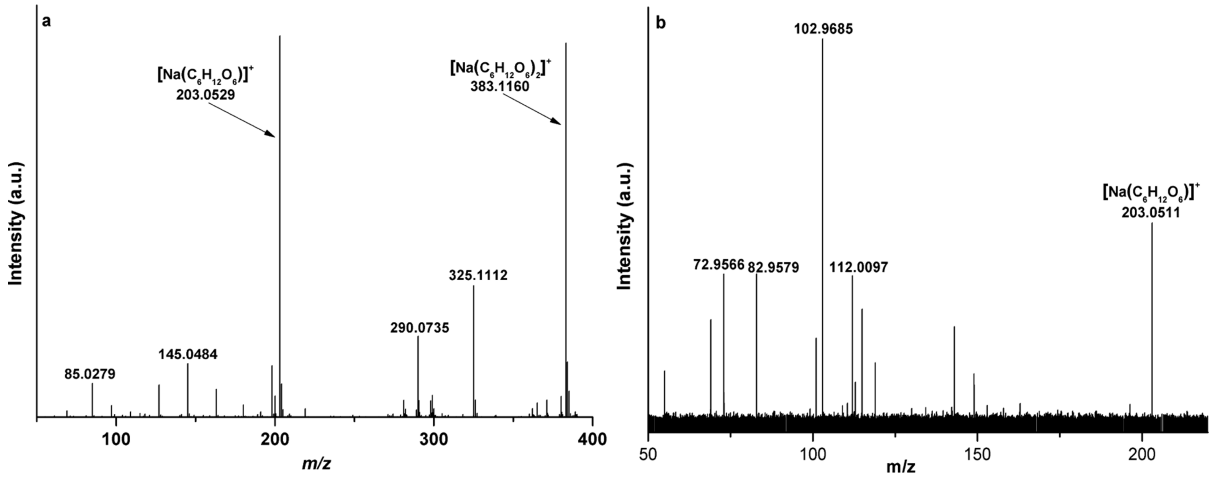

Figure 9. MS and MS/MS spectra of glucose in the absence of La(III). (a) MS spectrum. (b) MS/MS spectrum of the $[Na(C_6H_{12}O_6)]^+$ species with m/z of 203.0529, which was selected as target ion to conduct MS/MS experiment.

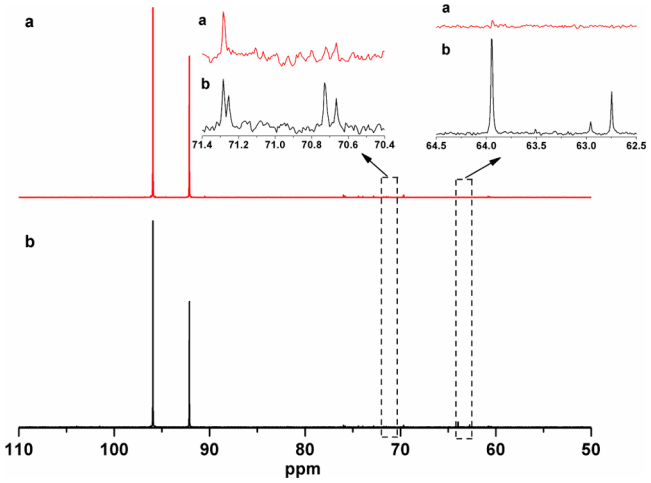

Figure 10. ^{13}C NMR spectra of the reactant solution in the absence (a) and presence (b) of La(III) (9.2 mmol/L) employing D-1-^{13}C-glucose (50.5 mmol/L) as the substrate in D_2O at 413 K for 1 h.

conversion of cellulose to EG and 1,2-PG, especially in terms of its practical application. For instance, La(III) can work effectively in this process at very low concentrations, and the price of the La(III) catalyst is only one-third of the tungstenic catalyst. The La(III) was only mildly basic, making it noncaustic toward the reactor equipment and nickel catalysts. The Ni–La(III) catalyst produced EG and 1,2-PG via two routes, effectively ensuring that all of the C6 molecules would be degraded into small C_2 and C_3 polyols. Although the stability of supported Ni–La(III) catalysts still needs further improving, such as by combining hydrothermally stable skeletal Ni catalysts with La(III), such an effective Ni–La(III) catalyst represents a promising candidate and inspiring strategy for the development of efficient catalysts for the conversion of cellulose to EG and 1,2-PG.

■ ASSOCIATED CONTENT

Supporting Information

The following file is available free of charge on the ACS Publications website at DOI: 10.1021/cs501372m.

Characterization of catalysts and reaction solution (ICP-AES, XRD, Q-TOF LC/MS and CO_2-TPD), Arrhenius curve and apparent activation energy of retro-aldol condensation of glucose with La(III), HPLC chromatograph of the D-(+)-glucose solution, and detailed computational results (PDF)

■ AUTHOR INFORMATION

Corresponding Authors

*E-mail: myzheng@dicp.ac.cn. Fax: (+86) 411-84691570.
*E-mail: dengwq@dicp.ac.cn.
*E-mail: taozhang@dicp.ac.cn.

Notes

The authors declare no competing financial interest.

■ ACKNOWLEDGMENTS

This work was supported by the National Nature Science Foundation of China (21376239, 21306191, and 21176235) and National Basic Research Program (973 program 2009CB226102). The authors thank Dr. Fan Yang for her kind help in Q-TOF LC/MS and NMR analysis.

■ REFERENCES

(1) Yabushita, M.; Kobayashi, H.; Fukuoka, A. *Appl. Catal., B* **2014**, *145*, 1–9.
(2) Delidovich, I.; Leonhard, K.; Palkovits, R. *Energy Environ. Sci.* **2014**, *7*, 2803–2830.
(3) Climent, M. J.; Corma, A.; Iborra, S. *Green Chem.* **2014**, *16*, 516–547.
(4) Klemm, D.; Heublein, B.; Fink, H.-P.; Bohn, A. *Angew. Chem., Int. Ed.* **2005**, *44*, 3358–3393.
(5) Rinaldi, R.; Schüth, F. *ChemSusChem* **2009**, *2*, 1096–1107.
(6) Vilcocq, L.; Castilho, P. C.; Carvalheiro, F.; Duarte, L. C. *ChemSusChem* **2014**, *7*, 1010–1019.
(7) Climent, M. J.; Corma, A.; Iborra, S. *Green Chem.* **2011**, *13*, 520–540.
(8) Geboers, J. A.; Van de Vyver, S.; Ooms, R.; Op de Beeck, B.; Jacobs, P. A.; Sels, B. F. *Catal. Sci. Technol.* **2011**, *1*, 714–726.
(9) Ruppert, A. M.; Weinberg, K.; Palkovits, R. *Angew. Chem., Int. Ed.* **2012**, *51*, 2564–2601.
(10) Fukuoka, A.; Dhepe, P. L. *Angew. Chem., Int. Ed.* **2006**, *45*, 5161–5163.
(11) Luo, C.; Wang, S.; Liu, H. *Angew. Chem., Int. Ed.* **2007**, *46*, 7636–7639.
(12) Yue, H.; Zhao, Y.; Ma, X.; Gong, J. *Chem. Soc. Rev.* **2012**, *41*, 4089–4089.

DOI: 10.1021/cs501372m
ACS Catal. 2015, 5, 874–883

(13) Ji, N.; Zhang, T.; Zheng, M.; Wang, A.; Wang, H.; Wang, X.; Chen, J. *Angew. Chem., Int. Ed.* **2008**, *47*, 8510−8513.
(14) Liu, Y.; Luo, C.; Liu, H. *Angew. Chem., Int. Ed.* **2012**, *51*, 3249−3253.
(15) Wang, A.; Zhang, T. *Acc. Chem. Res.* **2013**, *46*, 1377−1386.
(16) Zheng, M.; Pang, J.; Wang, A.; Zhang, T. *Chin. J. Catal.* **2014**, *35*, 602−613.
(17) Overview of World Fiber Production. http://dnfi.org/wp-content/uploads/2013/08/Portugal-Paper.pdf.
(18) Ji, N.; Zhang, T.; Zheng, M.; Wang, A.; Wang, H.; Wang, X.; Shu, Y.; Stottlemyer, A. L.; Chen, J. G. *Catal. Today* **2009**, *147*, 77−85.
(19) Tai, Z.; Zhang, J.; Wang, A.; Zheng, M.; Zhang, T. *Chem. Commun.* **2012**, *48*, 7052−7054.
(20) Zhang, Y.; Wang, A.; Zhang, T. *Chem. Commun.* **2010**, *46*, 862−864.
(21) Ji, N.; Zheng, M.; Wang, A.; Zhang, T.; Chen, J. G. *ChemSusChem* **2012**, *5*, 939−944.
(22) Zheng, M.; Wang, A.; Ji, N.; Pang, J.; Wang, X.; Zhang, T. *ChemSusChem* **2010**, *3*, 63−66.
(23) Zhao, G.; Zheng, M.; Wang, A.; Zhang, T. *Chin. J. Catal.* **2010**, *31*, 928−932.
(24) Zhao, G.; Zheng, M.; Zhang, J.; Wang, A.; Zhang, T. *Ind. Eng. Chem. Res.* **2013**, *52*, 9566−9572.
(25) Tai, Z.; Zhang, J.; Wang, A.; Pang, J.; Zheng, M.; Zhang, T. *ChemSusChem* **2013**, *6*, 652−658.
(26) Wang, X.; Meng, L.; Wu, F.; Jiang, Y.; Wang, L.; Mu, X. *Green Chem.* **2012**, *14*, 758−765.
(27) Xiao, Z.; Jin, S.; Pang, M.; Liang, C. *Green Chem.* **2013**, *15*, 891−895.
(28) Deuss, P. J.; Barta, K.; de Vries, J. G. *Catal. Sci. Technol.* **2014**, *4*, 1174−1196.
(29) Zhao, H.; Holladay, J. E.; Brown, H.; Zhang, Z. C. *Science* **2007**, *316*, 1597−1600.
(30) Choudhary, V.; Pinar, A. B.; Lobo, R. F.; Vlachos, D. G.; Sandler, S. I. *ChemSusChem* **2013**, *6*, 2369−2376.
(31) Choudhary, V.; Mushrif, S. H.; Ho, C.; Anderko, A.; Nikolakis, V.; Marinkovic, N. S.; Frenkel, A. I.; Sandler, S. I.; Vlachos, D. G. *J. Am. Chem. Soc.* **2013**, *135*, 3997−4006.
(32) Wang, Y.; Deng, W.; Wang, B.; Zhang, Q.; Wan, X.; Tang, Z.; Wang, Y.; Zhu, C.; Cao, Z.; Wang, G.; Wan, H. *Nat. Commun.* **2013**, *4* 10.1038/ncomms3141.
(33) Geboers, J.; Van de Vyver, S.; Carpentier, K.; de Blochouse, K.; Jacobs, P.; Sels, B. *Chem. Commun.* **2010**, *46*, 3577−3579.
(34) Zheng, X.; Lin, H.; Zheng, J.; Duan, X.; Yuan, Y. *ACS Catal.* **2013**, 2738−2749.
(35) Thyssen, V. V.; Maia, T. A.; Assaf, E. M. *Fuel* **2013**, *105*, 358−363.
(36) Zhi, G.; Guo, X.; Wang, Y.; Jin, G.; Guo, X. *Catal. Commun.* **2011**, *16*, 56−59.
(37) Kam, R.; Selomulya, C.; Amal, R.; Scott, J. *J. Catal.* **2010**, *273*, 73−81.
(38) Huang, Z.; Wang, X.; Wang, Z.; Zou, X.; Ding, W.; Lu, X. *RSC Adv.* **2014**, *4*, 14829−14832.
(39) Pang, J.; Wang, A.; Zheng, M.; Zhang, Y.; Huang, Y.; Chen, X.; Zhang, T. *Green Chem.* **2012**, *14*, 614−617.
(40) Liang, G.; He, L.; Arai, M.; Zhao, F. *ChemSusChem* **2014**, *7*, 1415−1421.
(41) Tajvidi, K.; Hausoul, P. J. C.; Palkovits, R. *ChemSusChem* **2014**, *7*, 1311−1317.
(42) Liang, G.; He, L.; Cheng, H.; Li, W.; Li, X.; Zhang, C.; Yu, Y.; Zhao, F. *J. Catal.* **2014**, *309*, 468−476.
(43) Huang, Z.; Chen, J.; Jia, Y.; Liu, H.; Xia, C.; Liu, H. *Appl. Catal., B* **2014**, *147*, 377−386.
(44) Sun, J. Y.; Liu, H. C. *Green Chem.* **2011**, *13*, 135−142.
(45) Saxena, U.; Dwivedi, N.; Vidyarthi, S. R. *Ind. Eng. Chem. Res.* **2005**, *44*, 1466−1473.
(46) Clark, I. T. *Ind. Eng. Chem.* **1958**, *50*, 1125−1126.
(47) Chambon, F.; Rataboul, F.; Pinel, C.; Cabiac, A.; Guillon, E.; Essayem, N. *ChemSusChem* **2013**, *6*, 500−507.
(48) Roman-Leshkov, Y.; Moliner, M.; Labinger, J. A.; Davis, M. E. *Angew. Chem., Int. Ed.* **2010**, *49*, 8954−8957.
(49) Assary, R. S.; Curtiss, L. A. *J. Phys. Chem. A* **2011**, *115*, 8754−8760.
(50) Román-Leshkov, Y.; Davis, M. E. *ACS Catal.* **2011**, *1*, 1566−1580.
(51) Bush, M. F.; Saykally, R. J.; Williams, E. R. *J. Am. Chem. Soc.* **2008**, *130*, 9122−9128.
(52) Kobayashi, S.; Nagayama, S.; Busujima, T. *J. Am. Chem. Soc.* **1998**, *120*, 8287−8288.
(53) Kobayashi, S. *Pure Appl. Chem.* **2007**, *79*, 235−245.
(54) Hayes, M. L.; Pennings, N. J.; Serianni, A. S.; Barker, R. *J. Am. Chem. Soc.* **1982**, *104*, 6764−6769.
(55) Gunther, W. R.; Wang, Y.; Ji, Y.; Michaelis, V. K.; Hunt, S. T.; Griffin, R. G.; Román-Leshkov, Y. *Nat. Commun.* **2012**, *3*, 1109.

DOI: 10.1021/cs501372m
ACS Catal. 2015, 5, 874−883